

Semi-automatic wavelet soft-thresholding applied to digital image error level analysis

Daniel C Jeronymo ^{Corresp. 1}

¹ Computer Engineering Department, Federal University of Technology - Paraná, Toledo, PR, Brazil

Corresponding Author: Daniel C Jeronymo
Email address: danielc@utfpr.edu.br

In this paper a method for detection of image forgery in lossy compressed digital images known as error level analysis (ELA) is presented and its noisy components are filtered with automatic wavelet soft-thresholding. With ELA, a lossy compressed image is recompressed at a known error rate and the absolute differences between these images, known as error levels, are computed. This method might be weakened if the image noise generated by the compression scheme is too intense, creating the necessity of noise filtering. Wavelet thresholding is a proven denoising technique which is capable of removing an image's noise avoiding altering other components, like high frequencies regions, by thresholding the wavelet transform coefficients, thus not causing blurring. Despite its effectiveness, the choice of the threshold is a known issue. However there are some approaches to select it automatically. In this paper, a lowpass filter is implemented through wavelet thresholding, attenuating error level noises. An efficient method to automatically determine the threshold level is used, showing good results in threshold selection for the presented problem. Standard test images have been doctored to simulate image tampering, error levels for these images are computed and wavelet thresholding is performed to attenuate noise. Results are presented, confirming the method's efficiency at noise filtering while preserving necessary error levels.

1 Semi-Automatic wavelet soft-thresholding 2 applied to digital image error level analysis

3 Daniel Cavalcanti Jeronymo¹

4 ¹Federal University of Technology - Paraná (UTFPR), Toledo Campus, Brazil

5 Corresponding author:

6 Daniel Cavalcanti Jeronymo¹

7 Email address: danielc@utfpr.edu.br

8 ABSTRACT

9 In this paper a method for detection of image forgery in lossy compressed digital images known as
10 error level analysis (ELA) is presented and its noisy components are filtered with automatic wavelet
11 soft-thresholding. With ELA, a lossy compressed image is recompressed at a known error rate and the
12 absolute differences between these images, known as error levels, are computed. This method might be
13 weakened if the image noise generated by the compression scheme is too intense, creating the necessity
14 of noise filtering. Wavelet thresholding is a proven denoising technique which is capable of removing
15 an image's noise avoiding altering other components, like high frequencies regions, by thresholding the
16 wavelet transform coefficients, thus not causing blurring. Despite its effectiveness, the choice of the
17 threshold is a known issue. However there are some approaches to select it automatically. In this paper,
18 a lowpass filter is implemented through wavelet thresholding, attenuating error level noises. An efficient
19 method to automatically determine the threshold level is used, showing good results in threshold selection
20 for the presented problem. Standard test images have been doctored to simulate image tampering, error
21 levels for these images are computed and wavelet thresholding is performed to attenuate noise. Results
22 are presented, confirming the method's efficiency at noise filtering while preserving necessary error
23 levels.

24 1 INTRODUCTION

25 Since late years, even before 1990, altering images digitally has become a disseminated practice, much
26 due to the personal computer popularization. For example, the number of tampered pictures, by definition
27 images where part of its original content has been some way altered, removed or combined with other
28 images, synthetic textures or even computer rendered graphics Lin et al. (2009), reached 10% of all photos
29 published in the United States around the year 1989 Amsberry (2009).

30 In addition, for a number of reasons, some of those are intended to deceive the viewer in ways that
31 hurt legal and moral principles guaranteed by law, creating a number of issues. The advent of powerful
32 tools with that purpose turns the detection in a very difficult process even for professionals.

33 The techniques for image forgery are many, Lin et al. (2009) names a few, such as, simple cutting
34 and pasting, known as cloning Ng and Chang (2004), matting for perfect blending Chuang et al. (2002);
35 Sun et al. (2004), graph cut for finding optimal composition boundaries Kwatra et al. (2003); Li et al.
36 (2004), texture synthesis Kwatra et al. (2003); Sun et al. (2005); Bugeau and Bertalmío (2009) and
37 variational approaches for synthesis of new content Bertalmío et al. (2000); Bugeau et al. (2010); Bugeau
38 and Bertalmío (2009); Pérez et al. (2003).

39 For that reason, techniques for detection of tampered images have attracted the attention of the
40 scientific community, current image forgery detection is achieved through either active or passive (blind)
41 approaches. Active approaches depend on the usage of watermarks or signatures Yu et al. (2005); Kong
42 et al. (2004); Amornraksa and Jantawongwilail (2006); Wang et al. (2008). On the other hand, passive
43 approaches do not need any explicit *a priori* information about the image, constituting a new direction
44 of great interest in the field of image forensics Mahdian and Saic (2009); Sloan and Hernandez-Castro
45 (2015). However, considering current art, there is no complete solution to automatically and blindly
46 determine image forgeries Lin et al. (2009).

47 Passive blind image forensics are well documented, featuring surveys such as Farid (2009b); Ng
48 et al. (2006). Current methods dwell on detecting cloning, which is essentially cutting and pasting in
49 an image Fridrich et al. (2003); Popescu and Farid (2004a); resampling, originated from processes of
50 resizing, rotating or stretching portions of pixels Popescu and Farid (2004b); Kirchner (2008); Mahdian
51 and Saic (2007); Prasad and Ramakrishnan (2006); splicing or matting, the process of combining two or
52 more images into a single composite, usually taking care to match borders Farid (1999); Ng and Chang
53 (2004) and statistical analysis, where statistical properties of natural images are exploited to detect image
54 manipulation Farid and Lyu (2003); Bayram et al. (2005, 2006); Mahdian and Saic (2009); Lin et al.
55 (2009).

56 Error level analysis (ELA) is a passive blind image forensic method created by Krawetz (2007),
57 although sometimes related to others authors due to failures in recent art Farid (2009a); Zhao et al. (2011)
58 to properly cite and acknowledge the original author of this method. This technique takes advantage of
59 lossy compression schemes of tampered images to detect forgeries.

60 Lossy compression schemes perform a trade off between data quality and compressed data size, at
61 first, this might seem as a drawback to a forensic analyst due to the loss of evidence associated with the
62 trade off, however, different quality levels in an image are evidence themselves.

63 An original image possesses an unique quality level, a property originated both from its acquisition
64 and compression scheme. When such an image is tampered, either through cloning, splicing or matting,
65 the original content is combined with foreign content, which will possess different quality levels, being
66 the original content usually already compressed and the foreign uncompressed.

67 ELA works by taking an image compressed with a lossy compression scheme, intentionally recom-
68 pressing at a known error rate and then computing the absolute difference between the first image and its
69 recompression.

70 This difference between images are the error levels associated with the original pixels, these error
71 levels, seen as an amount of change, are directly associated with compression loss.

72 If the amount of change is small, the pixel has reached its local minima for error at the determined
73 error rate, hence it is likely to be already compressed, on the other hand, if there is a large amount of
74 change, then the pixels were not at their local compression minima and are likely to be foreign Krawetz
75 (2007).

76 ELA's absolute differences are computed across all spatial frequencies in an image. This causes the
77 error levels to mimic the spatial frequencies of the pixels they represent. That is, low frequency regions,
78 regions where the tonal transition is smooth, such as uniform skies or skin, will present lower amounts of
79 change while high frequency regions, where the tonal transition is abrupt, such as fur, grass or hair, will
80 present higher amounts of change.

81 These fluctuations might confuse a forensic analyst, since both high frequency and foreign content
82 will present high amounts of change. Regarding this problem, a windowed absolute differences scheme
83 is presented in literature Farid (2009a) to compensate the fluctuations created by both low and high
84 frequencies.

85 Error levels are noisy by essence since the absolute differences are computed across all spatial
86 frequencies in the image. This causes the error levels to mimic the distribution of the spatial frequencies
87 present in the image, increasing the difficulty in the interpretation of error levels.

88 Noise, as any sharp changes in an image's intensity, implies in high-frequency components, thus,
89 lowpass filtering is a common application of noise removal in image analysis Seul et al. (2000). Several
90 convolution based methods of noise attenuation are present in image analysis literature such as Sun et al.
91 (1994); Nodes and Gallagher Jr. (1982); Dugad and Ahuja (1999); Gonzalez and Woods (2001); Lim
92 (1990); Gilboa et al. (2004); Salinas and Fernández (2007); Fernández et al. (2005); Bernardes et al.
93 (2010), however, the greatest downside of these methods is the blurring of images.

94 On the other hand, Wavelets thresholding is a process that uses a forward wavelet transform, filters
95 the noise by thresholding the resulting coefficients and then applying the inverse transform to recover the
96 image. It is able to effectively remove noise components without interfering with other signal components
97 present in an image, that is, without causing blurring Donoho (1993).

98 Although its success in image processing Arandiga et al. (2010); De Stefano et al. (2004); Heric and
99 Zazula (2007), determining the most adequate threshold level is a current issue because the thresholding
100 might affect components other than noise. With this issue in focus in recent wavelet thresholding literature,
101 several automatic and adaptive methods are proposed to determine the threshold, such as Deivalakshmi

102 and Palanisamy (2016); Ju et al. (2010); Yong and Qiang (2010); Liu et al. (2008); Madeiro et al. (2007);
 103 Poornachandra (2008); Wu et al. (2005); Chen et al. (2007); Zhang et al. (2002); Kovesi (1999), to cite a
 104 few.

105 In this paper, standard images such as the cameraman, farm, lena and peppers, are originally taken
 106 from a lossless compression format, TIFF, in 512x512 resolution and converted to a lossy compression
 107 format, JPEG, to simulate originally acquired images, i.e., from a camera. These images are then doctored
 108 to represent forgeries. Error levels are computed and the noise in them are removed using wavelet
 109 thresholding with its threshold automatically determined by the method presented in Kovesi (1999). A
 110 summary of the method is presented in Figure 1.

111 The results achieved show that the ELA technique is indeed very effective in detecting the forgeries
 112 and despite the noisy images generated in the ELA process, filtering through wavelet thresholding with
 113 automatic thresholding selection proved to be an effective approach in denoising, making easier to detect
 114 the forgeries. Therefore, the proposed method has its validity attested and could be used to diminish the
 115 attempts to moral rights by helping forensic professionals to detect a forged image.

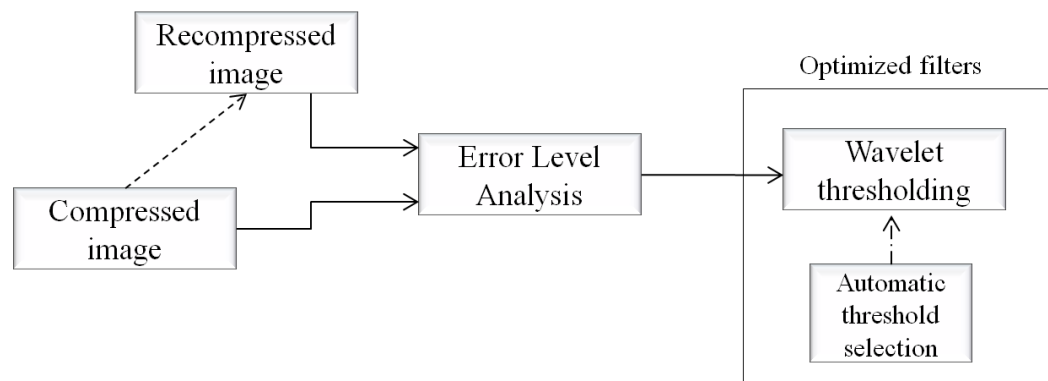


Figure 1. Summary and work flow of the method.

116 The rest of this paper is organized as follows: section 2 summarizes the proposed method, detailing the
 117 application of error level analysis, presenting standard test images, their doctored versions for this paper
 118 and the associated error levels; section 3 presents the process of wavelet thresholding and a scheme for
 119 automatic threshold selection; section 4 presents results obtained by the automatic wavelet thresholding;
 120 ultimately, in section 5, steps of the method are enumerated, its efficiency discussed and future works
 121 addressed.

122 2 ERROR LEVEL ANALYSIS

123 Error level analysis (ELA) is a passive blind image forensic method created by Krawetz Krawetz (2007)
 124 which takes advantage of the lossy compression schemes of tampered images to identify its forgery. The
 125 original quality level of a image is a unique feature itself, thus, any alteration process leaves its traces
 126 behind also in it. Briefly, ELA works by using an image compressed by a lossy scheme and recompressing
 127 it with a known error rate, then, it computes the absolute difference between the analyzed image and the
 128 recompressed one. Formally, ELA is described as follows.

Error levels, $ELA(n_1, n_2)$ where n_1 and n_2 are row and column indices, can be represented by

$$ELA(n_1, n_2) = |X(n_1, n_2) - X_{rc}(n_1, n_2)|, \quad (1)$$

for each color channel, where X is the image suspected of forgery and X_{rc} is the recompressed image. Total error levels are error levels averaged across all color channels, as in

$$ELA(n_1, n_2) = \frac{1}{3} \sum_{i=1}^3 |X(n_1, n_2, i) - X_{rc}(n_1, n_2, i)|, \quad (2)$$

129 where $i = 1, 2, 3$, for a RGB image.

130 This difference between images are the error levels associated with the original pixels, these error
 131 levels, seen as an amount of change, are directly associated with compression loss. If the amount of
 132 change is small, the pixel has reached its local minima for error at the determined error rate. However, if
 133 there is a large amount of change, then the pixels are not at their local minima and are likely to be foreign
 134 Krawetz (2007).

135 ELA's absolute differences are computed across all spatial frequencies in an image. This causes the
 136 error levels to mimic the spatial frequencies of the pixels they represent. That is, low frequency regions,
 137 regions where the tonal transition is smooth, such as uniform skies or skin, will present lower amounts of
 138 change while high frequency regions, where the tonal transition is abrupt, such as fur, grass or hair, will
 139 present higher amounts of change. These fluctuations might confuse a forensic analyst, since both high
 140 frequency and foreign content will present high amounts of change. Regarding this problem, a windowed
 141 absolute differences scheme is presented in literature Farid (2009a) to compensate the fluctuations created
 142 by both low and high frequencies.



Figure 2. Figure a) shows the original cameraman image, b) shows the forgery, with a zppelin in the background and c) shows ELA for the doctored image.

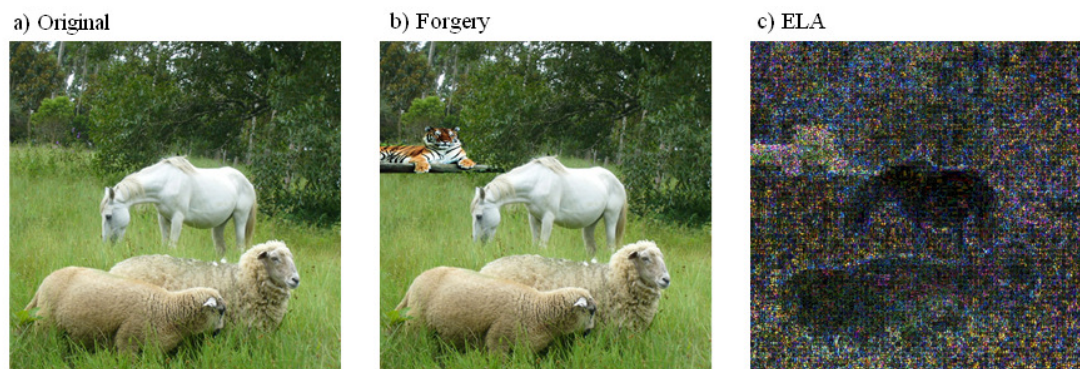


Figure 3. Figure a) shows the original farm image, b) shows the forgery, with a tiger in the background and c) shows ELA for the doctored image.

143 Figures 2,3,4,5 present the cameraman, farm, lena and peppers images, respectively. Exhibited in
 144 these figures are the original and doctored images. ELA is presented for the doctored images in the
 145 512x512 resolution. Figure 2 shows ELA's weakness in gray-scale images, since the level of information
 146 is lower, so are the precision of error levels, thus, error levels created by high frequency components and
 147 error levels created by different qualities are indistinguishable. This problem is not present in any of the
 148 color images.



Figure 4. Figure a) shows the original lena image, b) shows the forgery, with a flower on her hat and contrast enhanced eyes and lips and c) shows ELA for the doctored image.

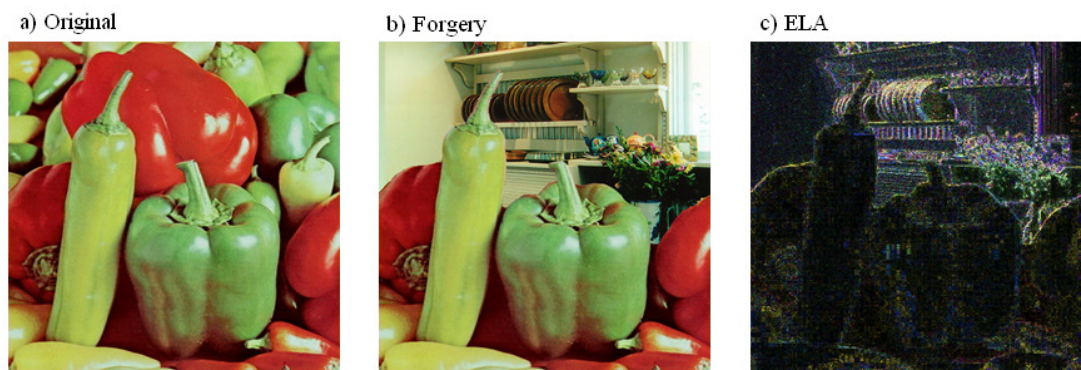


Figure 5. Figure a) shows the original peppers image, b) shows the forgery, with a kitchen on the background and c) shows ELA for the doctored image.

149 3 AUTOMATIC WAVELET THRESHOLD SELECTION

150 Wavelet thresholding, also known as wavelet shrinkage, is the process of converting a signal to a time-scale
 151 domain through a forward wavelet transform, wavelet coefficients are then thresholded according to a
 152 certain criteria and the reverse wavelet transform converts the wavelet coefficients back to the time-space
 153 domain of the image.

154 Wavelets have proved very efficient at separating signal and noise, although no particular wavelet has
 155 been shown to be more effective at denoising than others, however, threshold choice is a delicate issue.
 156 Here is presented a short review of the method described in Kovesi (1999) to automatically determine the
 157 threshold.

158 In Kovesi (1999), the Rayleigh distribution is utilized for estimation of the magnitude of response
 159 vectors in *log Gabor* filters, considering 2D Gaussian noise in the complex plane. This distribution is
 160 defined by

$$R(x) = \frac{x}{\sigma_g^2} e^{-\frac{x^2}{2\sigma_g^2}}, \quad (3)$$

161 where σ_g^2 is the variance of the 2D Gaussian distribution which describes the position of the filter's
 162 response vectors. The mean of this distribution is

$$\mu_r = \sigma_g \sqrt{\frac{\pi}{2}}, \quad (4)$$

163 and the variance is

$$\sigma_r^2 = \frac{4 - \pi}{2} \sigma_g^2. \quad (5)$$

164 Threshold choice is then a matter of choosing a value which is a scale of the standard deviation beyond
 165 the mean noise, as in

$$T = \mu_r + k \cdot \sigma_r, \quad (6)$$

166 where k controls how beyond the noise's mean is the standard deviation.

167 A reliable estimate of the mean of noise amplitude distribution can be determined by

$$E(A_N) = \frac{1}{2} \sqrt{\frac{-\pi}{\ln(\frac{1}{2})}} \cdot \text{median}, \quad (7)$$

168 where A_N is the N 'th wavelet transform of the image. Smallest scales of A_N provide the best result, since
 169 they contain the most noise, further discussion can be seen in Kovesi (1999). In fact, noise power is
 170 elevated at small scales Xu et al. (1994), at it can be seen in the wavelet decomposition of the cameraman
 171 error levels, in Figure 6. That shows the wavelet scales decomposition, it is clear that at small scales seen
 172 in the smaller images in the upper left side the noise is greater than the larger scales.

173 The noise mean μ_r is effectively equal to $E(A_N)$ and the variance, σ_r can be calculated by combining
 174 equation 5 with

$$\sigma_g = \frac{E(A_N)}{\sqrt{\frac{\pi}{2}}}, \quad (8)$$

175 resulting in

$$\sigma_r = \frac{(4 - \pi) \cdot E(A_N)}{\pi}. \quad (9)$$

176 This statistical approach to the estimation of the threshold, T , through equation 6, proves successful
 177 in removing noise from wavelet transforms.

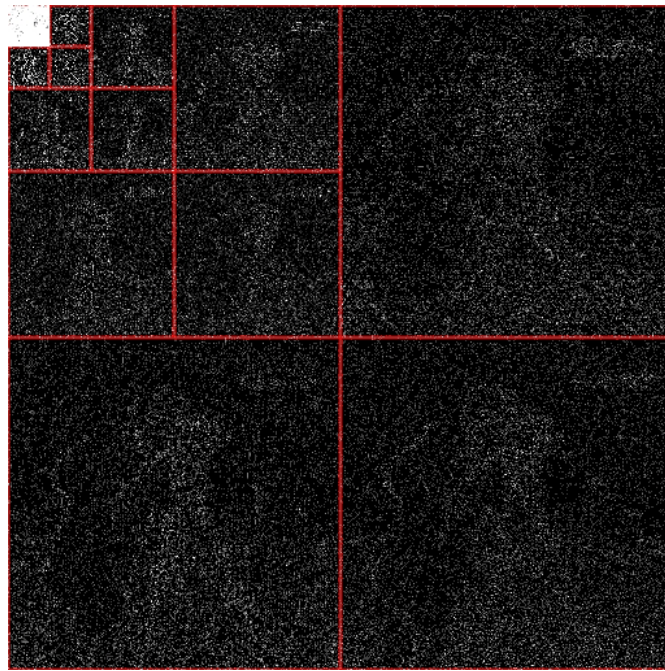


Figure 6. Wavelet decomposition of the cameraman error levels, showing greater noise power in small scales.

4 RESULTS

178

179 Soft-thresholding is utilized to ensure avoiding the introduction of frayed edges, typical of wavelet
180 thresholding. The standard test images have been wavelet shrunk with the automatic threshold selection
181 described in the previous section. The orthogonal Daubechies wavelet with a vanishing moment of four
182 was used for the wavelet transforms.

183

For the cameraman image, results are presented in figure 7. Despite ELA's failure to distinguish
184 between the low resolution error levels in the gray scale image, the noise removal results are adequate.
185 The value of the k scale factor used for this image was 4.

186

For the farm image, results are presented in figure 8. Overall noise has been greatly attenuated and the
187 tiger stands out from the background. However, high frequency spatial characteristics of the image such
188 as the vegetation increase error levels throughout the entire image.

189

For the lena image, results are presented in figure 9. The image's interpretation is difficult due to error
190 levels created from the high frequency features such as the fur, however, the flower stands out. Minor
191 modifications such as the contrast enhanced eyes and lips are not distinguishable.

192

For the peppers image, results are presented in figure 10. This image presents the best results in
193 both noise removal and error level identification. The kitchen at the background completely stands out,
194 canceling the peppers at the front.

5 CONCLUSION

195

196 This paper presents the not well known method Error Level Analysis, correctly identifying its original
197 author despite omission in recent literature, and investigates the usage of wavelet transforms in error level
198 noise removal. A method to automatically select a threshold level is used, from Kovese (1999), showing
199 good results in this application.

200

Standard images such as the cameraman, farm, lena and peppers, are doctored to represent forgeries.
201 These images are then studied with error level analysis and compared with the error level analysis of
202 lower resolutions of these same images. It's noted that ELA fails to process gray scale images due to low
203 resolution of error levels but graciously succeeds in color images.

204

205 Afterwards, noise removal is performed, through wavelet thresholding, transforming the images from
the time-space representation to time-scale, filtering the noise through wavelet's coefficients thresholding,



Figure 7. The cameraman image has been wavelet thresholded with a k scale of 4.

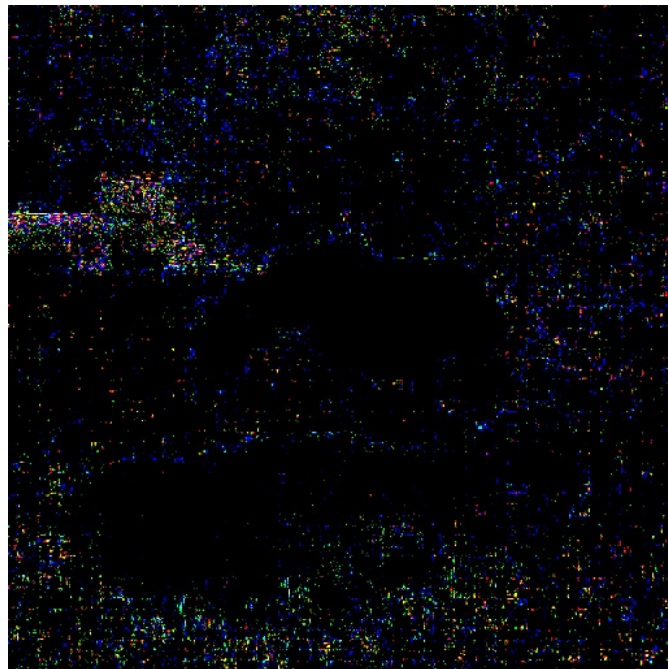


Figure 8. The farm image has been wavelet thresholded with a k scale of 6.

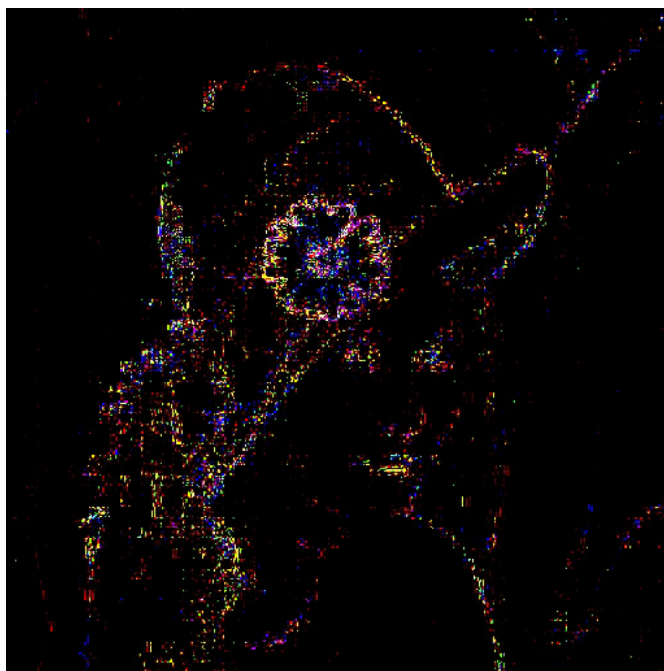


Figure 9. The lena image has been wavelet thresholded with a k scale of 8.

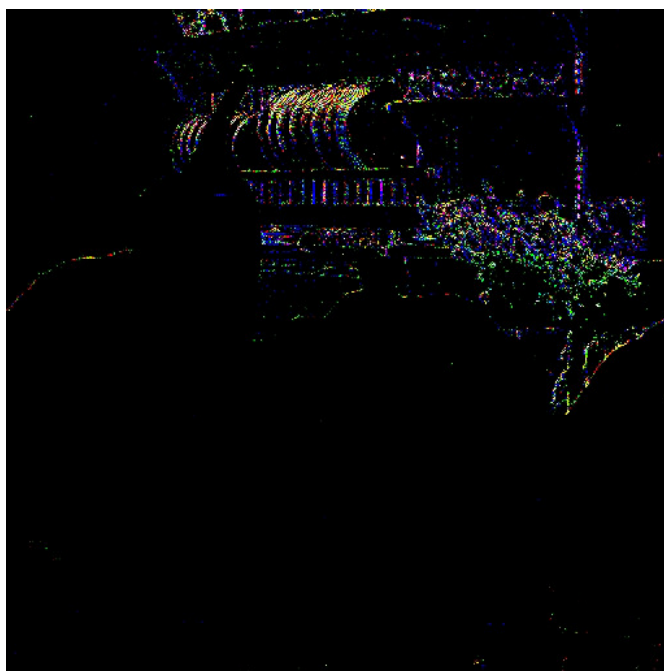


Figure 10. The peppers image has been wavelet thresholded with a k scale of 20.

206 where the threshold value is statistically calculated from the image, and performing the reverse wavelet
207 transform on the image.

208 Empirically, results show the approach successfully attenuates noise and improves error levels, better
209 identifying regions of the image where tampering has occurred.

210 REFERENCES

- 211 Amornraksa, T. and Jantawongwilail, K. (2006). Enhanced images watermarking based on amplitude
212 modulation. *Image and Vision Computing*, 24(2):111–119.
- 213 Amsberry, C. (2009). Alterations of photos raise host of legal, ethical issues. *The Wall Street Journal*,
214 pages Section B, 1.
- 215 Arandiga, F., Cohen, A., Donat, R., and Matei, B. (2010). Edge detection insensitive to changes of
216 illumination in the image. *Image and Vision Computing*, 28(4):553–562.
- 217 Bayram, S., Avcibas, I., Sankur, B., and Memon, N. (2005). Image manipulation detection with binary
218 similarity measures. In *in Proceedings of Conference of European Signal Processing*, Antalya, Turkey.
- 219 Bayram, S., Avcibas, I., Sankur, B., and Memon, N. (2006). Image manipulation detection. *Journal of*
220 *Electronic Imaging*, 15.
- 221 Bernardes, R., Maduro, C., Serranho, P., Araújo, A., Barbeiro, S., and Cunha-Vaz, J. (2010). Improved
222 adaptive complex diffusion despeckling filter. *Opt. Express*, 18(23):24048–24059.
- 223 Bertalmío, M., Sapiro, G., Caselles, V., and Ballester, C. (2000). Image inpainting. In *SIGGRAPH*, pages
224 417–424, New Orleans, Louisiana, USA.
- 225 Bugeau, A. and Bertalmío, M. (2009). Combining texture synthesis and diffusion for image inpainting.
226 In *VISAPP 2009 - Proceedings of the Fourth International Conference on Computer Vision Theory and*
227 *Applications, Lisboa, Portugal, February 5-8, 2009 - Volume 1*, pages 26–33, Lisbon, Portugal.
- 228 Bugeau, A., Bertalmío, M., Caselles, V., and Sapiro, G. (2010). A comprehensive framework for image
229 inpainting. *IEEE Transactions on Image Processing*, 19(10):2634–2645.
- 230 Chen, Y., Lei, L., Ji, Z.-C., and Sun, J.-F. (2007). Adaptive wavelet threshold for image denoising by
231 exploiting inter-scale dependency. In Huang, D.-S., Heutte, L., and Loog, M., editors, *Advanced Intelli-*
232 *gent Computing Theories and Applications. With Aspects of Theoretical and Methodological Issues*,
233 volume 4681 of *Lecture Notes in Computer Science*, pages 869–878. Springer Berlin / Heidelberg.
- 234 Chuang, Y. Y., Agarwala, A., Curless, B., Salesin, D. H., and Szeliski, R. (2002). Video matting of
235 complex scenes. In *Proceedings of the 29th annual conference on Computer graphics and interactive*
236 *techniques*, SIGGRAPH '02, pages 243–248, San Antonio, Texas. ACM.
- 237 De Stefano, A., White, P. R., and Collis, W. B. (2004). Film grain reduction on colour images using
238 undecimated wavelet transform. *Image and Vision Computing*, 22(11):873–882.
- 239 Deivalakshmi, S. and Palanisamy, P. (2016). Removal of high density salt and pepper noise through
240 improved tolerance based selective arithmetic mean filtering with wavelet thresholding. *{AEU} -*
241 *International Journal of Electronics and Communications*, 70(6):757 – 776.
- 242 Donoho, D. L. (1993). Nonlinear wavelet methods for recovery of signals, densities, and spectra from
243 indirect and noisy data. In *In Proceedings of Symposia in Applied Mathematics*, pages 173–205.
244 American Mathematical Society.
- 245 Dugad, R. and Ahuja, N. (1999). Video denoising by combining kalman and wiener estimates. In *Proc.*
246 *of the International Conference on Image Processing(ICIP)*, pages 152–156, Kobe, Japan.
- 247 Farid, H. (1999). Detecting digital forgeries using bispectral analysis. Technical report, MIT AI Memo
248 AIM-1657, MIT.
- 249 Farid, H. (2009a). Exposing digital forgeries from jpeg ghosts. *Trans. Info. For. Sec.*, 4:154–160.
- 250 Farid, H. (2009b). A survey of image forgery detection. *IEEE Signal Processing Magazine*, 2(26):16–25.
- 251 Farid, H. and Lyu, S. (2003). Higher-order wavelet statistics and their application to digital forensics.
252 *Computer Vision and Pattern Recognition Workshop*, 8:94.
- 253 Fernández, D. C., Salinas, H. M., and Puliafito, C. A. (2005). Automated detection of retinal layer
254 structures on optical coherence tomography images. *Opt. Express*, 13(25):10200–10216.
- 255 Fridrich, A. J., Soukal, B. D., and Lukáš, A. J. (2003). Detection of copy-move forgery in digital images.
256 In *in Proceedings of Digital Forensic Research Workshop*, Cleveland, Ohio, USA.
- 257 Gilboa, G., Member, S., Sochen, N., and Zeevi, Y. Y. (2004). Image enhancement and denoising
258 by complex diffusion processes. *IEEE Transactions on Pattern Analysis and Machine Intelligence*,
259 26:1020–1036.

- 260 Gonzalez, R. C. and Woods, R. E. (2001). *Digital Image Processing*. Addison-Wesley Longman
261 Publishing Co., Inc., Boston, MA, USA, 2nd edition.
- 262 Heric, D. and Zazula, D. (2007). Combined edge detection using wavelet transform and signal registration.
263 *Image and Vision Computing*, 25(5):652–662.
- 264 Ju, H., Shijing, W., and Jiantao, L. (2010). Application of wavelet transform threshold in the de-noising of
265 fiber optic gyroscopes. In *Systems and Control in Aeronautics and Astronautics (ISSCAA), 2010 3rd
266 International Symposium on*, pages 1165–1168, Harbin, China.
- 267 Kirchner, M. (2008). Fast and reliable resampling detection by spectral analysis of fixed linear predictor
268 residue. In *in ACM Multimedia and Security Workshop*, pages 11–20, Oxford, UK.
- 269 Kong, X. W., Liu, Y., Liu, H. J., and Yang, D. L. (2004). Object watermarks for digital images and video.
270 *Image and Vision Computing*, 22(8):583–595.
- 271 Kovese, P. (1999). Phase preserving denoising of images. In *The Australian Pattern Recognition Society
272 Conference: DICTA'99*, pages 212–217, Perth WA. ACM.
- 273 Krawetz, N. (2007). A picture's worth... digital image analysis and forensics. Technical report, Black Hat
274 Briefings, USA.
- 275 Kwatra, V., Schödl, A., Essa, I., Turk, G., and Bobick, A. (2003). Graphcut textures: image and video
276 synthesis using graph cuts. *ACM Trans. Graph.*, 22:277–286.
- 277 Li, Y., Sun, J., Tang, C.-K., and Shum, H.-Y. (2004). Lazy snapping. *ACM Trans. Graph.*, 23:303–308.
- 278 Lim, J. S. (1990). *Two-dimensional signal and image processing*. Prentice-Hall, Inc., Upper Saddle River,
279 NJ, USA.
- 280 Lin, Z., He, J., Tang, X., and Tang, C.-K. (2009). Fast, automatic and fine-grained tampered jpeg image
281 detection via dct coefficient analysis. *Pattern Recognition*, 42:2492–2501.
- 282 Liu, C., Szeliski, R., Kang, S. B., Zitnick, C. L., and Freeman, W. T. (2008). Automatic estimation and
283 removal of noise from a single image.
- 284 Madeiro, J. P. V., Cortez, P. C., Oliveira, F. I., and Siqueira, R. S. (2007). A new approach to qrs
285 segmentation based on wavelet bases and adaptive threshold technique. *Medical Engineering &
286 Physics*, 29(1):26–37.
- 287 Mahdian, B. and Saic, S. (2007). On periodic properties of interpolation and their application to image
288 authentication. In *Information Assurance and Security, International Symposium on*, pages 439–446,
289 Los Alamitos, CA, USA. IEEE Computer Society.
- 290 Mahdian, B. and Saic, S. (2009). Using noise inconsistencies for blind image forensics. *Image Vision
291 Computing*, 27:1497–1503.
- 292 Ng, T. T. and Chang, S. F. (2004). Blind detection of photomontage using higher order statistics. In *in
293 IEEE International Symposium on Circuits and Systems*, pages 688–691, Vancouver, Canada.
- 294 Ng, T. T., Chang, S. F., Lin, C. Y., and Sun, Q. (2006). Passive-blind image forensics. In *In Multimedia
295 Security Technologies for Digital Rights*.
- 296 Nodes, T. and Gallagher Jr., N. (1982). Center weighted median filters: Some properties and their
297 applications in image processing. *IEEE Transactions on Acoustics, Speech and Signal Processing*,
298 30(5):739–746.
- 299 Pérez, P., Gangnet, M., and Blake, A. (2003). Poisson image editing. *ACM Transactions on Graphics
300 (SIGGRAPH'03)*, 22(3):313–318.
- 301 Poornachandra, S. (2008). Wavelet-based denoising using subband dependent threshold for ecg signals.
302 *Digital Signal Processing*, 18(1):49–55.
- 303 Popescu, A. C. and Farid, H. (2004a). Exposing digital forgeries by detecting duplicated image regions.
304 Technical report, Department of Computer Science, Dartmouth College.
- 305 Popescu, A. C. and Farid, H. (2004b). Exposing digital forgeries by detecting traces of re-sampling. *IEEE
306 Transactions on Signal Processing*, 53:758–767.
- 307 Prasad, S. and Ramakrishnan, K. R. (2006). On resampling detection and its application to image
308 tampering. In *IEEE International Conference on Multimedia and Exposition*, pages 1325–1328,
309 Toronto, Canada. IEEE.
- 310 Salinas, H. M. and Fernández, D. C. (2007). Comparison of PDE-Based Nonlinear Diffusion Approaches
311 for Image Enhancement and Denoising in Optical Coherence Tomography. *IEEE Transactions on
312 Medical Imaging*, 26(6).
- 313 Seul, M., O'Gorman, L., and Sammon, M. J. (2000). *Practical algorithms for image analysis: description,
314 examples, and code*. Cambridge University Press, New York, NY, USA.

- 315 Sloan, T. and Hernandez-Castro, J. (2015). Forensic analysis of video steganography tools. *PeerJ*
316 *Computer Science*, 1:e7.
- 317 Sun, J., Jia, J., Keung Tang, C., and Yeung Shum, H. (2004). Poisson matting. *ACM Transactions on*
318 *Graphics*, 23:315–321.
- 319 Sun, J., Yuan, L., Jia, J., and Shum, H.-Y. (2005). Image completion with structure propagation. *ACM*
320 *Trans. Graph.*, 24:861–868.
- 321 Sun, T., Gabbouj, M., and Neuvo, Y. (1994). Center weighted median filters: Some properties and their
322 applications in image processing. *Signal Processing*, 35(3):213–229.
- 323 Wang, X., Hou, L., and Wu, J. (2008). A feature-based robust digital image watermarking against
324 geometric attacks. *Image and Vision Computing*, 26(7):980–989.
- 325 Wu, Y., He, Y., and Cai, H. (2005). Optimal threshold selection algorithm in edge detection based on
326 wavelet transform. *Image and Vision Computing*, 23(13):1159 – 1169.
- 327 Xu, Y., Weaver, J., Healy, D., and Lu, J. (1994). Wavelet transform domain filters: a spatially selective
328 noise filtration technique. *IP*, 3(6):747–758.
- 329 Yong, T. and Qiang, W. (2010). The realization of wavelet threshold noise filtering algorithm in dsp. In
330 *Measuring Technology and Mechatronics Automation (ICMTMA), 2010 International Conference on*,
331 volume 3, pages 953 –956, Changsha, China.
- 332 Yu, L. J., Niu, X. M., and Sun, S. H. (2005). Print-and-scan model and the watermarking countermeasure.
333 *Image and Vision Computing*, 23(9):807–814.
- 334 Zhang, S., Wong, M.-Y., and Zheng, Z. (2002). Wavelet threshold estimation of a regression function
335 with random design. *Journal of Multivariate Analysis*, 80(2):256 – 284.
- 336 Zhao, Y. Q., Shih, F. Y., and Shi, Y. Q. (2011). Passive detection of paint-doctored jpeg images. In
337 *Proceedings of the 9th international conference on Digital watermarking, IWDW'10*, pages 1–11,
338 Berlin, Heidelberg. Springer-Verlag.